The effects of meteorological parameters and diffusive barrier reuse on the sampling rate of a passive air sampler for gaseous mercury

David S. McLagan,[1] Carl P. J. Mitchell,[1] Haiyong Huang,[1] Batual Abdul Hussain,[1] Ying Duan Lei,[1] Frank Wania[1,*]

[1] Department of Physical and Environmental Sciences, University of Toronto Scarborough, 1065 Military Trail, M1C 1A4, Toronto, Ontario, Canada

* Corresponding Author – email: frank.wania@utoronto.ca; phone: +1 416-287-7225

ABSTRACT

13   Passive air sampling of gaseous mercury (Hg) requires a high level of accuracy to discriminate

14   small differences in atmospheric concentrations. Meteorological parameters have the potential

15   to decrease this accuracy by impacting the sampling rate (SR), i.e., the volume of air that is

16   effectively stripped of gaseous mercury per unit of time. We measured the SR of a recently

17   calibrated passive air sampler for gaseous Hg in the laboratory under varying wind speeds

18   (wind-still – 6 m s^{-1}), temperatures (-15 – 35 °C), and relative humidities (44 – 80%). While

19   relative humidity has no impact on SR, SR increases slightly with both wind speed (0.003 m^3

20   day^{-1} increase in SR or 2.5% of the previously calibrated SR for every m s^{-1} increase for wind

21   speeds > 1 m s^{-1}, typical of outdoor deployments) and temperature (0.001 m^3 day^{-1} increase in

22   SR or 0.7% for every 1 °C increase). The temperature dependence can be fully explained by the

23   effect of temperature on the molecular diffusivity of gaseous mercury in air. Although these

24   effects are relatively small, accuracy can be improved by adjusting SRs using measured or

25   estimated temperature and wind speed data at or near sampling sites. We also assessed the

26   possibility of reusing Radiello® diffusive barriers previously used in the passive air samplers. The

27   mean rate of gaseous Hg uptake was not significantly different between new and previously

28   used diffusive barriers in both lab and outdoor deployments, irrespective of the applied

29   cleaning procedure. No memory effect from Radiellos® previously deployed in a high Hg

30   atmosphere was observed. However, a loss in replicate precision for the dirtiest Radiellos® in

31   the indoor experiment suggests that cleaning is advisable prior to reuse.

KEYWORDS

33   Passive air sampling, Hg, atmosphere, calibration, green chemistry

1. INTRODUCTION

34

35 Fine spatial resolution measurements of atmospheric contaminants are difficult and expensive,

36 especially at remote locations and in developing countries. By allowing for simultaneous, cost-

37 effective measurements at a multitude of sites, passive air samplers (PASs) are useful,

38 complementary monitoring tools in atmospheric science. PASs can be deployed in high

39 numbers, at sites away from sources of electricity, and in locations where the costs and logistics

40 of active sampler deployments can be prohibitive (McLagan et al., 2016a). In order for a PAS to

41 yield volumetric air concentration data, a sampling rate (SR), i.e., the volume of air that is

42 effectively stripped of the contaminant of concern per unit of time, needs to be derived. This is

43 done either in calibration experiments that deploy the PAS concurrently with reliable active

44 sampling techniques or theoretically based on an understanding of the processes controlling

45 mass transfer from atmosphere to PAS sorbent (Armitage et al., 2013; Gustin et al., 2011; Skov

46 et al., 2007). Any uncertainty and bias in the SR is directly propagated to the volumetric air

47 concentration derived from a PAS. Accordingly, a reliable PAS requires that the impact of

48 various factors influencing the SR is, in order of preference, either eliminated, minimized or

49 quantifiable and predictable.

50 A common conceptual model of uptake in PASs assumes a stagnant air layer or air-side

51 boundary layer (ASBL) around the sorbent, through which contaminant transfer occurs solely by

52 molecular diffusion (McLagan et al., 2016a; Shoeib and Harner, 2002). Wind decreases the

53 thickness of the ASBL which in turn increases the SR (Bartkow et al., 2005; Moeckel et al., 2009;

54 Pennequin-Cardinal et al., 2005). Diffusive barriers aim to reduce the influence of wind by

55 standardizing the molecular diffusion distance to the sorbent and thereby ensuring that the

56 diffusive component of contaminant transfer is the rate limiting step (Huang et al., 2014;

57 Lozano et al., 2009; McLagan et al., 2016a). For PASs with diffusive barriers the ASBL is shifted

58 from the outside of the sorbent to the outside of the diffusive barrier (McLagan et al., 2016b).

59 While a diffusive barrier thus reduces the relative contribution of the ASBL to the overall

60 diffusion distance, it cannot entirely mitigate SR variability caused by wind (Pennequin-Cardinal

61 et al., 2005; Plaisance et al., 2002; Skov et al., 2007). Protective shields around the sorbent or

62 diffusive barrier are often employed to further reduce the influence of wind by reducing the

63 face velocities at these surfaces. However, like diffusive barriers, they too are not likely to

64 completely eliminate the influence of wind on the thickness of the ASBL (Huang et al., 2014).

65 Temperature has the potential to affect SR in two ways: (i) changing the rate of gas phase

66 diffusion of the contaminant due to the temperature dependence of molecular diffusion

67 coefficients (Armitage et al., 2013; Huang et al., 2014; Lozano et al., 2009); and (ii) shifting the

68 partitioning equilibria between the sorbent and the gas phase (Armitage et al., 2013; Lozano et

69 al., 2009; McLagan et al., 2016a). Relative humidity (RH) may affect SRs by influencing the

70 sorptive properties of certain sorbents for target analytes (Huang et al., 2014). Other factors

71 that may affect the sorption of contaminants to PAS sorbents include passivation of sorbents

72 (interfering compounds blocking sorbent uptake sites or stripping analytes through reaction)

73 (Brown et al., 2012; Gustin et al., 2011), degradation of the sorbent over time (Brown et al.,

74 2011; McLagan et al., 2016a), and uptake of the contaminant to the sampler housing or

75 diffusive barrier (Gustin et al., 2011; Huang et al., 2014; McLagan et al., 2016a).

76 Mercury is a persistent, bioaccumulative, and toxic contaminant of global concern that has

77 come under greater international scrutiny with the adoption of the Minamata Convention

78 (UNEP, 2013). A key stipulation under Article 19 of the convention "Research, Development and

79 Monitoring" is the requirement of participating parties to improve current monitoring networks

80 (UNEP, 2013). A PAS for measuring atmospheric Hg could play an important role in this context,

81 if it can be shown to be suitable for monitoring long-term background concentrations,

82 concentration gradients in and around Hg sources, and personal exposure levels (McLagan et

83 al., 2016a). Gaseous elemental Hg (GEM) is generally the dominant form of atmospheric Hg

84 (typically making up >95%), due to its high atmospheric residence time of ~1 year (Driscoll et

85 al., 2013; Pirrone et al., 2010; Selin, 2009), especially at sites remote from combustion sources

86 (McLagan et al., 2016a; Peterson et al., 2009; Rutter et al., 2009). The long atmospheric

87 residence time of GEM results in fairly uniform background concentrations within each

88 hemisphere, with much of the global atmosphere having levels within <25% of the hemispheric

89 average (Gustin et al., 2011). PASs capable of discriminating such small concentration variability

90   require high accuracy and precision, i.e. *SR*s need to be well characterized and repeatable.

91   Existing PASs for gaseous mercury have struggled to achieve the accuracy and precision

92   necessary for background monitoring due to inadequate detection limits or highly variable SRs

93   (Huang et al., 2014; McLagan et al., 2016a).

94   We recently introduced a PAS for gaseous Hg with a precision based uncertainty of 2 ± 1 % that

95   uses an activated carbon sorbent and a Radiello® diffusive barrier (McLagan et al., 2016b).

96   While it is believed that the sampler takes up predominantly GEM, we cannot rule out the

97   possibility for gaseous oxidized Hg to also pass through the diffusive barrier (McLagan et al.,

98   2016b). We therefore use the term gaseous Hg to define the target analyte. An earlier

99   calibration of this PAS at one outdoor location yielded a *SR* of 0.121 m^3 day^{-1} (McLagan et al.,

100   2016b). Here we report on a series of laboratory experiments that quantified the effect of wind

101   speed, temperature, and RH on the *SR* of that sampler. We additionally explored the possibility

102   of reusing the Radiello® diffusive barrier in multiple deployments in order to further reduce the

103   costs associated with the sampler's use. During deployment, the inside of the Radiello® can

104   become covered in sorbent dust. It is also possible that atmospheric components, e.g.

105   atmospheric particulate matter and oxidants, sorb to or react with the diffusive barrier during

106   deployment. Thus, in addition to meteorological impacts on the PAS's SR, we also explored the

107   effect of prior use and cleaning of the diffusive barrier on the uptake of Hg in the PAS.

108   **2. METHODS**

109   **2.1 Sampler Design**

110   The sampler consists of a porous stainless steel mesh cylinder, filled with ~0.7 g of sulphur-

111   impregnated activated carbon sorbent (HGR-AC; Calgon Carbon Corp.), which is inserted into a

112   Radiello® radial diffusive body (Sigma Aldrich), which itself is placed inside a polyethylene-

113   terephthalate protective jar. During deployments the opening of the jar, covered with a

114   polypropylene (PP) mesh screen, is facing down. After sampling the jar is sealed with a PP cap

115   and PTFE tape for transport and storage. McLagan et al. (2016b) provide more detail on the PAS

116   design.

2.2 Study Design

2.2.1 WIND. PAS in four different configurations were exposed to different wind conditions in the laboratory at the University of Toronto Scarborough: (1) regular, white Radiello® with windshield, (2) white Radiello® without windshield, (3) thick-walled, less porous, yellow Radiello® with windshield, and (4) yellow Radiello® without windshield. Adopting the experimental setup of Zhang et al. (2013), electronic fans (Delta Electronics Inc., model number: BFC1212B) were employed to generate wind for each individual sampler. The angle of wind incidence was always 90°, i.e. we simulated wind that is blowing parallel to the surface. Wind speeds of 1, 1.5, 2, 3, 4, 5, and 6 m s^{-1} were achieved by manipulating the distance between PASs and fan (see Fig. S1 and Fig. S2). Wind speeds for each individual PAS were measured every 5 seconds with a hot-wire Anemometer/Thermometer (Traceable®, VWR International) for five minutes before and five minutes after each deployment. As such, average wind speeds of individual samplers within each wind speed treatment varied slightly (Fig. 1). "Wind-still" experiments without fans were performed for comparison (with wind speed assumed to be 0.05 m s^{-1}).

While experiments with white Radiellos (configuration 1 and 2) generally lasted one week, additional experiments lasting two, three, and four weeks were performed at selected wind speeds (3 and 6 m s^{-1}). Experiments with yellow Radiellos (configurations 3 and 4) lasted two weeks (the lower *SR* of yellow Radiello® requires longer deployment times to reach detection limits) and were only performed at wind speeds of 3 and 6 m s^{-1}, as well as without fans. Additionally, a 3 months uptake experiment under wind-still conditions was performed in order to obtain a precise *SR* of the PAS with a white Radiello deployed indoors with a protective shield. Eighteen samplers were deployed at the same time and triplicates were removed after 15, 28, 46, 56, 70 and 84 days. The earlier indoor calibration experiment described in McLagan et al. (2016b) had been performed without a windshield.

Temperature and RH, monitored before, after, and periodically during each individual experiment, ranged from 21.9 – 24.2 °C and from 32 – 53%. While there was some variation in

144   the gaseous Hg concentration as recorded by the Tekran 2537A between deployments, the

145   average concentration across all wind experiments was 1.9 ± 0.3 ng m^{-3}.

146   *2.2.2 TEMPERATURE & RELATIVE HUMIDITY.* The regular PAS configuration (configuration 1)

147   was exposed to eight different combinations of temperature and RH (Table 1) for two weeks

148   periods in climate controlled walk-in chambers located at the Biotron Facility of Western

149   University in London, Ontario. Each experiment was replicated five times. Samplers were

150   attached to metal shelving units near the centre of the chambers where a continuous flow of

151   air from the outflow of the climate control units of $1.1 - 2.3$ m s^{-1} was observed using the hot-

152   wire Anemometer over a two minute period at the completion of each experiment. The

153   average actively measured gaseous Hg concentration across all temperature and RH

154   experiments was 2.2 ± 0.9 ng m^{-3}.

155   **Table 1: Combinations of temperature and relative humidity during the eight experiments performed**
156   **in climate-controlled chambers**

Temp (°C)	-15.0±0.1	5.0±0.0	12.5±0.1	19.9±0.0	20.0±0.1	20.0±0.1	27.5±0.0	35.0±0.0
RH%	68±1	77±1	76±2	44±5	60±1	80±0	60±1	45±3

157

158   *2.2.3 RADIELLO® REUSE.* The potential impacts of sorbent dust accumulation or atmospheric

159   contamination during prolonged deployment periods on sampling rates and therefore on the

160   ability to reuse the Radiello® diffusive barriers are unknown. Currently, new diffusive barriers

161   are used for each deployment. In this experiment, previously used Radiellos® were redeployed

162   after different cleaning procedures were applied. Six cleaning treatments were applied: *new*

163   (unused Radiellos®), *uncleaned* (unaltered after previous deployments), *physical* (physical

164   agitation with funnel brushes and compressed air blow down), *soap* (Citranox® detergent,

165   cleaning brushes, and deionized water, compressed air blow down, deionized water rinse and

166   sonication and air drying), *acid* (six hour soak in 20% HNO$_3$ bath, deionized water rinse,

167   compressed air blow down, deionized water rinse and sonication and air drying), and *heat-acid*

168   (six hour soak in 20% HNO$_3$ bath at 40 °C, deionized water rinse, compressed air blow down,

169   deionized water rinse and sonication and air drying). Prior to cleaning, diffusive bodies were

170   categorized based on the extent of visible dust coating using a 5 point scale (0 – new, 1 – very

171   low, 2 – low, 3 – moderate, 4 – high, and 5 – very high). To the extent this was possible with a

172   limited stock of previously deployed Radiellos®, we evenly distributed Radiellos® of variable

173   dust coating among the treatments (see Table S1 for details). We also tested Radiellos®

174   previously deployed in contaminated environments with very high gaseous Hg concentrations

175   (~100 – 10000 ng m^{-3}) to assess whether such deployments led to a memory effect whereby

176   sorbed Hg is released from the diffusive body during subsequent uses. All samplers from this

177   *memory* treatment contained moderate dust coating and were not cleaned.

178   Five replicate samplers for each of the 7 treatments were deployed for a period of two weeks in

179   a laboratory with slightly elevated Hg concentrations (previously measured as ~5-10 ng m^{-3}) at

180   the University of Toronto Scarborough. Additionally, five different replicate samplers for each

181   of the three treatments *new*, *uncleaned*, and *soap* were exposed for 34 days outdoors on the

182   campus of the University of Toronto Scarborough (43.78714 °N, 79.19049 °W). In this case, all

183   previously used Radiellos® were heavily dust coated (category 4 or 5, see Table S2 for details).

184   In both the indoor and outdoor experiment all samplers were deployed concurrently.

185   Therefore, no active gaseous Hg measurements were necessary and the mass of sorbed Hg

186   could be directly compared and was used in data analysis.

187   *2.2.4 ACTIVE GASEOUS MERCURY MEASUREMENTS.* A Tekran 2537A (Tekran Instruments Corp.)

188   was used to measure the gaseous Hg concentrations at 5 min intervals throughout all wind,

189   temperature and RH experiments. A sampling inlet that combined a 2 m Teflon tube connected

190   to a 0.2 μm PTFE filter was used (detailed setup is given in: (Cole and Steffen, 2010; Steffen et

191   al., 2008)). Auto-calibrations were made using the internal Hg permeation unit every 25 hrs and

192   these were verified through manual injections from a Tekran 2505 Mercury Vapor Primary

193   Calibration Unit (Tekran Instruments Corp.) before and after each set of experiments. Quality

194   control and assurance of the Tekran 2537A data sets followed the Environment Canada

195   Research Data Management and Quality Control system (Steffen et al., 2012).

196   *2.2.5 SAMPLING RATE CALCULATION. SRs* (m^3 day^{-1}) were calculated using:

197    $$SR = {m}/{(C\ t)} \qquad\qquad (1)$$

198   where m is the mass of sorbed mercury (ng), C is the concentration of gaseous Hg measured by

199   the Tekran 2537A (ng m^{-3}), and t is the deployment time of the PAS (days). With the exception

200   of the 3-months experiment, the *SR*s were derived from single point calibrations using Eq. (1).

201   *SR*s derived from a single deployment have a higher uncertainty than *SR*s derived from

202   experiments involving multiple simultaneous deployments of variable length, such as those

203   described in McLagan et al. (2016b). This uncertainty is further increased when deployment

204   times are short and gaseous Hg concentrations are low, as m will be closer to quantification

205   limits. To nevertheless constrain the uncertainties from the experiments described here, we

206   performed a high number of replications. In the wind experiments, true replication was not

207   possible, as wind speed varied slightly between each deployment. While they cannot be called

208   replicates, we performed a very large number of individual experiments, which allowed for the

209   derivation of a robust relationship between *SR* and wind speed. Additionally, the variable length

210   of the experiments at selected wind speeds not only added to the number of data points, but

211   also allowed us to assess if there was any effect of deployment time on *SR*.

212   **2.3 Analyses**

213   Total Hg (THg) in the activated carbon sorbent was quantified using thermal combustion,

214   amalgamation, and atomic absorption spectroscopy in oxygen (O_2) carrier gas (USEPA Method

215   7473) using an AMA254 (Leco Instruments Ltd.) (USEPA, 2007). Because the sorbent in a PAS

216   cannot be assumed to take up Hg homogeneously, the entire carbon from each PAS was

217   analyzed in two aliquots of up to 0.45 g each. In order to increase the lifetime of AMA254

218   catalyst tubes while processing samples with high sulphur content, catalyst tubes were

219   amended with 5 g of sodium carbonate (Na_2CO_3) and ~ 0.15 g of Na_2CO_3 was added directly to

220   each sample boat (McLagan et al., submitted). Samples were dried for 30 seconds at 200 °C and

221   thermally decomposed at 750 °C for 330 seconds, while gaseous elemental Hg was trapped on

222   the gold amalgamator. After combustion the system was purged for 60 seconds to ensure all

223 pyrolysis gases were removed from the catalyst. Throughout the analysis the catalyst was

224 heated to 550 °C. After purging, the amalgamator was heated to 900 °C for 12 seconds to

225 release the trapped Hg into the cuvette where absorption at 253.65 nm was measured by dual

226 detector cells for both low and high absolute amounts of Hg.

227 The instrument was calibrated by adding varying amounts of Hg liquid standard for AAS (1000 ±

228 5 mg l^{-1}; in 10% w/w HCl; Inorganic Ventures) to ~0.22 g of clean (unexposed) HGR-AC. ~0.15 g

229 of Na_2CO_3 was added on top of the liquid standard and HGR-AC. In all experiments absolute

230 amounts of Hg were less than 20 ng and the high cell was therefore not required for

231 quantification. The low cell calibration included standards of 0, 0.1, 0.25, 0.5, 1, 2.5, 5, 10, 15,

232 and 20 ng of Hg (uncertainty in autopipette is 1 ± 0.004 ng) fitted with a linear relationship.

233 **2.4 Quality Assurance and Control**

234 Both analytical and field blanks were included in all experiments. Analytical blanks represented

235 analyses of clean HGR-AC with mean concentration of 0.3 ± 0.2 ng g^{-1} of HGR-AC (n=14). Field

236 blanks, taken both at the start and end of each experiment, were taken to the site, opened,

237 deployed, and then immediately taken down, sealed and stored for analysis. The mean field

238 blank concentration for the wind experiments (n=7), the temperature/RH experiments (n=5),

239 and the Radiello® reuse experiments (n=4) were 0.5 ± 0.2 ng g^{-1}, 0.58 ± 0.15 ng g^{-1} and 0.38 ±

240 0.08 ng g^{-1} of HGR-AC, respectively. All results are blank adjusted by subtracting the mean field

241 blank concentration for each experiment multiplied by the mass of HGR-AC in that sample.

242 Analytical precision was monitored throughout the experiments (approximately every 10-15

243 instrumental runs) by analyzing 5 or 10 ng Hg liquid Standards for AAS added to ~0.22 g of HGR-

244 AC. Recoveries for precision testing were 100.1 ± 1.6 (n=62), 100.0 ± 1.3 (n=24), and 100.0 ± 1.3

245 (n=21) % for the wind, temperature/RH, and reuse experiments, respectively. Recovery was

246 monitored throughout the experiments (approximately every 10-15 runs) by analyzing a high

247 sulphur, bituminous coal standard reference material, NIST 2685c (S = 5 wt%; National Institute

248 of Standards and Technology), or our own in-house reference material, RM-HGR-AC1

249 (powdered HGR-AC loaded with Hg by exposure to air for four months then homogenized; 23.1

250 ± 0.8 ng g^{-1} based on 198 analytical runs). Recoveries of NIST 2685c were 101 ± 3 (n=35), 102 ±

251 3 (n=14), and 99 ± 4 (n=10) % for the wind, temperature/RH, and reuse experiments,

252 respectively. Recoveries of RM-HGR-AC1 were 98 ± 3 (n=43), 97 ± 2 (n=13), and 96 ± 2 (n=10) %

253 for the wind, temperature/RH, and reuse experiments, respectively. All statistical tests were

254 either performed by hand or using R v3.3.2 (R Foundation for Statistical Computing).

255 **3.   RESULTS AND DISCUSSION**

256 **3.1 Wind**

257 The effect of wind speed on SR varied considerably across the four tested PAS configurations

258 (Fig. 1). The greatest effect was observed for white Radiello® without windshield (configuration

259 2), which is a configuration that is unlikely to be used in practice. A positive linear relationship

260 across the tested wind speed range (wind still to 6 m s^{-1}) had a slope indicative of a 0.022 m^3

261 day^{-1} (or 18% of the calibrated SR) increase in SR for every 1 m s^{-1} increase in wind speed (Fig.

262 1). Previous investigators, using the white Radiello® (without protective shield) to monitor

263 varying atmospheric contaminants, fitted logarithmic (Pennequin-Cardinal et al., 2005;

264 Plaisance, 2011; Skov et al., 2007) or quadratic (Plaisance et al., 2004) relationships to data

265 describing the effect of wind speed on SR. The SR was most sensitive at lower wind speeds.

266 However, due to the limited number or range of measured wind speeds, or high data

267 uncertainty, a linear relationship fits some of these data equally well (McLagan et al., 2016a).

268 The addition of the windshield (configuration 1), which is the current method of practice,

269 reduced the effect of wind speed on the SR, particularly at higher wind speeds. The best fit of

270 the data was a logarithmic relationship (linear fit: R^2 = 0.66) in which SR was most sensitive to

271 wind speed between 0 and 1 m s^{-1} (Fig. 1). While average wind speeds of less than 1 m s^{-1} are

272 common for indoor deployments, outdoors average wind speeds typically exceed 1 m s^{-1} (98.3%

273 of data from 0° 10' resolution global data set of monthly averaged wind speeds at 10 m above

274 ground level between 1961 and 1990 (New et al., 2002)). When we consider only the data >1 m

275 s^{-1} we observe a slight, but significant, positive linear relationship between SR and wind speed

276 (p=0.006) corresponding to a 0.003 m^3 day^{-1} (or 2.5% or the previously calibrated SR) increase

277 in *SR* for every m s^{-1} increase in wind speed (Fig. 1). Neither configuration with the thicker,

278 yellow Radiello® led to a significant effect of wind speed on *SR* (Fig. 1). With the protective

279 shield in place the *SR* was approximately 10% lower than without the protective shield.

280 Plaisance (2011) also noted a negligible effect of wind speed on *SR* using a yellow Radiello® PAS

281 without any protective shield when monitoring benzene.

282
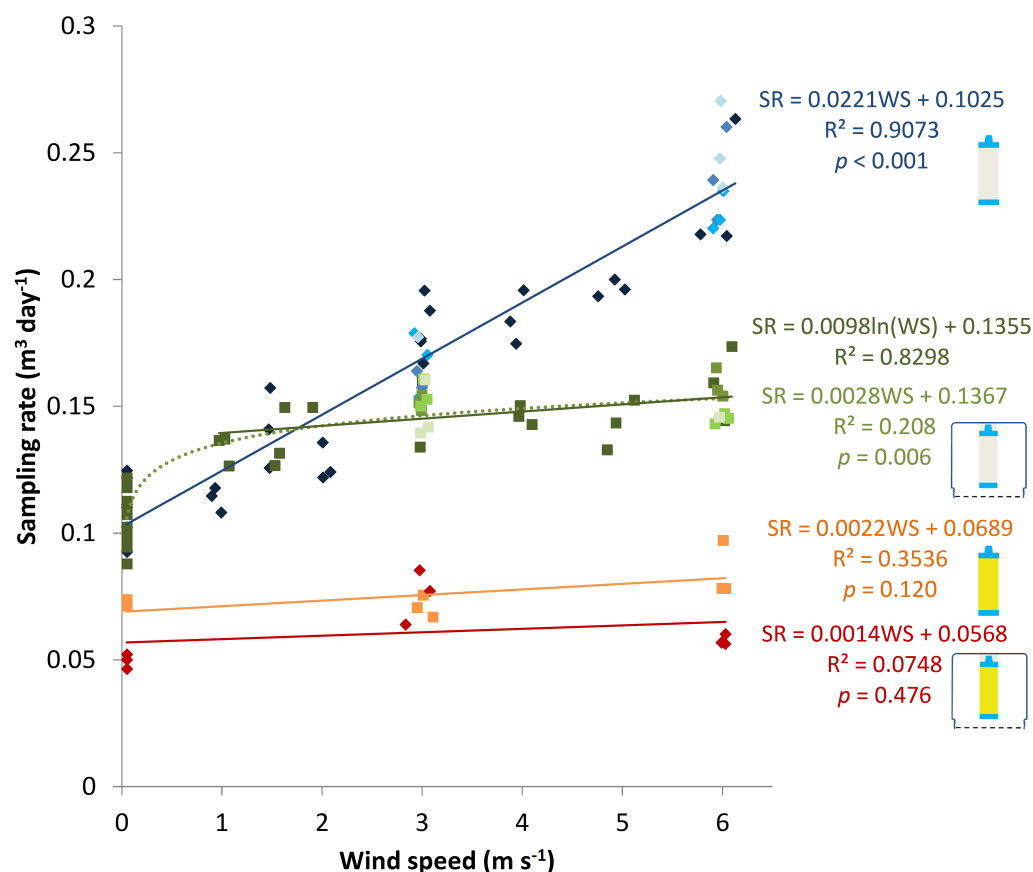
283 **Figure 1: The effect of wind speed on the sampling rate of four different configurations of a passive air**
284 **sampler for gaseous mercury. Configuration 1: White Radiello®, with protective shield (1 week: ■, 2**
285 **week: ■, 3 week: ■, and 4 week: ■ deployments); Configuration 2: White Radiello®, without**
286 **protective shield (1 week: ♦, 2 week: ♦, 3 week: ♦, and 4 week: ♦ deployments); Configuration 3:**
287 **Yellow Radiello®, with protective shield (■); Configuration 4: White Radiello®, without protective**
288 **shield (♦). Sampling rate, wind speed relationships are based on all data for each configuration**
289 **irrespective of deployment length.**

290 The importance of a diffusive barrier is illustrated by the very strong effect of wind speed on

291 the *SR* of another PAS for gaseous Hg that also utilizes an activated carbon sorbent, but has no

292   diffusive barrier: the SR increased by 0.126 m^3 day^{-1} (or 97% of the calibrated SR) for every m s^{-1}

293   increase in wind speed (Guo et al., 2014; Zhang et al., 2012). This information and the results

294   here demonstrate the merit of employing both diffusive barriers and protective shield in

295   reducing the effect of wind speed on SR. The diffusive path length of the PAS has three

296   components: (1) the ASBL, (2) the diffusive barrier (adjusted for the porosity of the diffusive

297   barrier), and (3) the internal airspace of the Radiello® (McLagan et al., 2016b). Employing a

298   thicker, less porous diffusive barrier (yellow Radiello®) increases the diffusive path length of the

299   diffusive barrier component, in turn reducing the SR. By reducing turbulence on the outside of

300   the diffusive barrier, the protective shield essentially increases the thickness of the ASBL

301   (McLagan et al., 2016b), leading to a reduction in SR.

302   Because the samplers were not exposed to exactly the same wind speeds, it is not possible to

303   construct uptake curves from the experiments with variable deployment length. It is, however,

304   possible to test whether the measured SRs depend on the length of the single point

305   calibrations. The relationship between deployment length and SR was not significant ($p > 0.05$),

306   irrespective of the applied wind speed (wind-still, ~3 m s^{-1}, and ~6 m s^{-1}) or configuration (1 and

307   2); see Fig. S3 for details. This confirms that the SRs derived from short one-week deployments

308   were neither biased high or low.

309   The 3-month uptake experiment under wind-still conditions produced a SR of 0.106 ± 0.009 m^3

310   day^{-1} when calculated as the average of single point calibrations (see Fig. S4 for uptake curve).

311   The slope of the regression of m against $C*t$ (McLagan et al., 2016b; Restrepo et al., 2015) gave

312   a very similar SR of 0.109 ± 0.009 m^3 day^{-1}. Because the latter method is thought to give a

313   slightly more reliable SR (McLagan et al., 2016b; Restrepo et al., 2015), we suggest to use this

314   SR for indoor deployments of the PAS using the white Radiello and a windshield (configuration

315   1). This SR is 9.9% lower than the SR obtained in an earlier outdoor calibration study, despite

316   the higher temperature (~23°C) indoors than outdoors (mean temperature across all

317   deployments: 7.6°C). Additionally, the replicate precision of samplers from this uptake

318   experiment for the wind-still data with the protective shield (11 ± 8%) was significantly poorer

319   ($p < 0.001$) than in the outdoor calibration study with the same sampler setup (2 ± 1.3%; mean

320   wind speed 1.89 m s^{-1}) (McLagan et al., 2016b). Both the lower *SR* and the greater uncertainty

321   of the *SR* are consistent with the effect of wind observed for this configuration (green markers

322   in Fig. 1): At the low wind speeds of indoor deployments (< 1 m s^{-1}), the *SR* is expected to be

323   both lower and more sensitive to changes in wind speed. Although, conditions for this

324   experiment were labelled "wind-still", in reality any activity within the laboratory (movement of

325   lab personnel, opening and closing of doors, etc.) will result in small variations in wind speeds

326   around the PAS within the range where the *SR* is most sensitive to such variations (Zhang et al.,

327   2013).

3.2 Temperature and relative humidity

329   Relative humidity, tested at 44, 60, and 80% and a stable temperature of 20 °C, had no

330   significant effect on *SR* (p = 0.080; see Fig. S5). It is therefore appropriate to analyze the effect

331   of temperature on *SR* despite small variations in RH at different temperature levels. We

332   observed a significant, positive, linear relationship between *SR* and temperature (p < 0.001; Fig.

333   2) corresponding to a 0.001 m^3 day^{-1} increase in *SR* for every 1 °C increase in temperature (or

334   0.7% of the calibrated *SR*). This relationship remained linear across the tested range from -15 to

335   35 °C.

336   Temperature can affect the *SR* because of its impact on (i) the partitioning equilibrium between

337   the sorbent and the gas phase and (ii) the diffusion coefficient (McLagan et al., 2016a;

338   Pennequin-Cardinal et al., 2005). The uptake capacity of the HGR-AC for gaseous Hg is

339   extremely high and we suspect that any change in the sorption equilibrium caused by changing

340   temperatures should have a negligible effect on the SR. The increase in diffusivity caused by an

341   increase in temperature is easily quantified. Fig. 2 also displays *SR* as a function of temperatures

342   predicted with a previously described model based on Fick's first law of diffusion (McLagan et

343   al., 2016b). While the predicted *SR*s are ~8% lower than the measured ones, the slope of the

344   relationship between *SR* and temperature is the same (no significant difference, z-score test, *p*

345   = 0.427), confirming that the effect of temperature on the diffusivity of gaseous Hg is sufficient

346   to explain the observed temperature dependence of the *SR*.

347
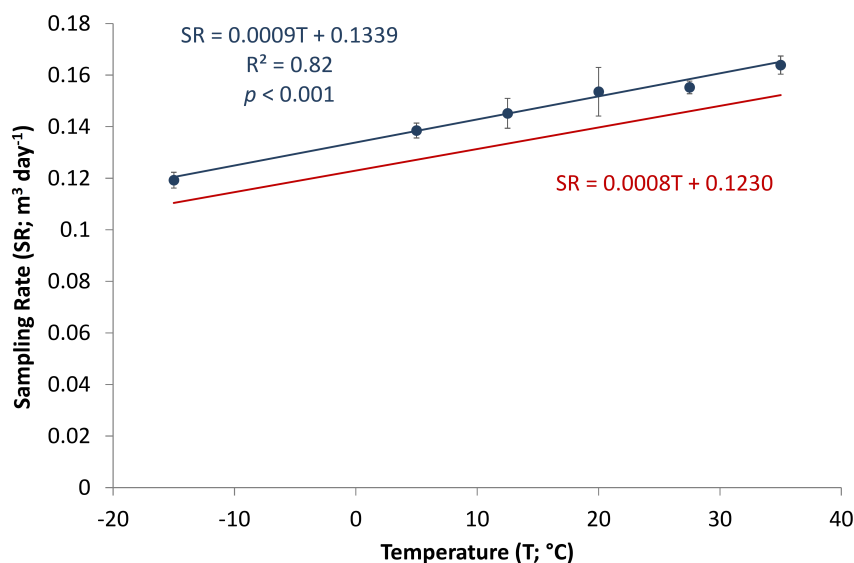
Figure 2: The effect of temperature on the sampling rate of a passive air sampler for gaseous mercury as determined experimentally (blue) and as calculated using the diffusion model (red) by McLagan et al. (2016b). The measured and calculated temperature dependence, given by the slopes of the relationships, are not significantly different.

Earlier studies on PAS for gaseous Hg did not observe an effect of temperature on SR. Guo et al. (2014) found no significant effect of temperature on the SR of their activated carbon based PAS between -10 and 35 °C. Similarly, there was no effect of temperature on the SR of a PAS using a solid gold sorbent and a white Radiello® diffusive body (Skov et al., 2007). In neither case, however, was the precision of the measurement sufficient to detect the small dependence of SR on temperature caused by the effect of temperature on diffusivity. Such a small temperature effect can only be detected in a highly precise sampler.

3.3 Radiello® reuse

In the Radiello® reuse experiment conducted indoors, no significant difference in the amount of sorbed Hg was observed between *new*, *uncleaned*, or any of the cleaned Radiellos® (ANOVA, p = 0.467; Fig. 3(A)). Similarly, when we ignore the effect of cleaning, no significant difference in the sorbed amount of Hg was observed between Radiellos® with different degrees of dust coatings, including the new Radiellos® (ANOVA, p = 0.841; Fig. 3(B)). The cleaning treatments also did not differ in terms of the observed variances (Levene's Test, p = 0.307). However, the

366 amount of Hg taken up in Radiellos® with the most dust (category 5) had a significantly higher

367 variance than all other treatments (p = 0.004, Levene's Test with Tukey's Honest Significant

368 Difference post hoc test). Although the differences between all Radiello® treatments in the

369 indoor Radiello® reusability experiments are small, the significantly higher variability observed

370 for Radiellos® with the highest dust coating suggests some form of cleaning would be better in

371 maintaining the high level of precision of this PAS. Effect size, using Cohen's d value (see S5),

372 was then applied to examine differences in treatments without the use of traditional binary

373 hypotheses testing (See Table S3). In comparison to new Radiellos® *soap*, *acid*, and *heat-acid*

374 were the most effective treatments. While there was no significant difference in means

375 (ANOVA; p = 0.548) or variances (Levene's; p = 0.221) for the outdoor experiment testing *new*,

376 *uncleaned*, and *soap* Radiellos®, effect size analysis (see S5) confirmed that *soap* cleaning is an

377 effective method in preparing used Radiellos® for redeployment (Fig. 4(C)).
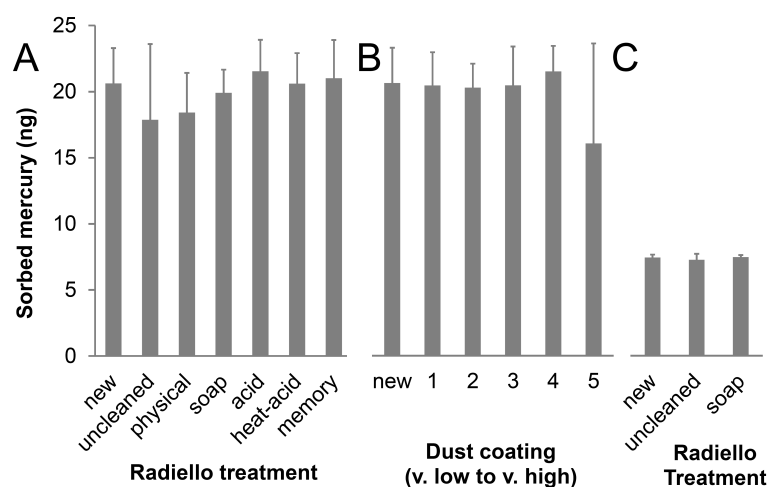
378

379 **Figure 3: Mean sorbed mercury for differing Radiello® cleaning treatments and at varying degrees of**
380 **HGR-AC dust coating inside the Radiello® (Panel B) from indoor experiment. Cleaning treatments and**
381 **degree of dust coating is described in Sect. 2.2.3. Panel A also includes the memory effect treatment,**
382 **which were uncleaned Radiellos® from deployments in a high concentration environment. Panel C**
383 **presents the mean sorbed mercury for differing Radiello® cleaning treatments from outdoor**
384 **experiment.**

385 Uptake of Hg in uncleaned Radiellos® previously deployed in gaseous Hg concentrations 2 – 4

386 orders of magnitude higher than the other Radiellos® (*memory* treatment) was also not

387 significantly different from any of the other treatments in terms of mean (ANOVA: p = 0.499) or

388   variance (Levene's: p = 0.307; Fig. 3(A)). This implies that very little Hg was sorbed to the

389   Radiello® and re-released during the subsequent deployment and that gaseous Hg has little

390   affinity for the porous high-density polyethylene diffusive membrane of the Radiello®.

391   **4.   RECOMMENDATIONS AND CONCLUSIONS**

392   While the SR of the PAS in its standard configuration (white Radiello® with protective shield)

393   was found to depend on both wind speed and temperature, the effects are both small and

394   predictable. The accuracy of volumetric air concentrations derived from the PAS can be

395   improved by applying adjustment factors to the SR, especially for deployments at or close to

396   background gaseous Hg concentrations. The SR of the standard configuration PAS (white

397   Radiello® with shield) deployed outdoors of 0.121 m^3 day^{-1} was obtained for a mean wind

398   speed of 1.89 m s^{-1} and a mean temperature of 7.6°C.[15] We recommend to use the increments

399   from Fig. 1 and Fig. 2, i.e. 0.003 m^3 day^{-1} increase in SR for every m s^{-1} increase in wind speed

400   and 0.001 m^3 day^{-1} increase in SR for every 1 °C increase in temperature to adjust the SR of

401   0.121 m^3 day^{-1} to the average temperature and wind speed of each PAS deployment (See S6 for

402   SR adjustment equation and sample calculation).

403   The experiments here predict a SR of 0.142 m^3 day^{-1} for an average wind speed of 1.89 m s^{-1}

404   (Fig. 1) and a SR of 0.141 m^3 day^{-1} for an average temperature of 7.6°C (Fig. 2). Both these

405   values are greater than the SR of 0.121 m^3 day^{-1} from the calibration study (McLagan et al.,

406   2016b). While we presently do not know the reason for this discrepancy, it may be related to

407   the relatively short deployment periods used in the present experiments. As mentioned above,

408   short deployment at background concentrations yield a SR with a higher uncertainty. Also,

409   McLagan at al. (2016b) observed that SR for PAS deployed outdoors for less than 1-2 months

410   were higher than the SR derived for the entire one-year sampling period. Despite this slight

411   discrepancy, we note that the y-intercepts of the relationships reported here (the magnitude of

412   the SR) are less important than their slopes (i.e. the temperature and wind speed adjustment

413   factors). An ongoing study measuring the uptake of gaseous Hg in PAS deployed at several

414   locations with widely different temperature and wind speed conditions will help refine both the

415   *SR* applicable to outdoor deployments and the validity of the laboratory derived adjustment

416   factors for temperature and wind speed reported here.

417   When designing a PAS, there is a need to strike a balance between maximizing the *SR* and

418   minimizing the variability in the *SR* caused by factors such as wind speed, objectives that are

419   contradictory in nature (McLagan et al., 2016a). Although using a thicker, yellow Radiello® with

420   or without a protective shield are the methods least affected by wind, the *SR* for these methods

421   is approximately half that of the white Radiello® with a shield. A lower *SR* translates to lower

422   amounts of sorbed Hg, which means that longer deployments are required to reach method

423   quantification limits (MQL). The PAS configuration with white Radiello® and windshield needs

424   to be exposed to typical background concentrations of gaseous Hg (~1.5 – 2 ng m^{-3}) for

425   approximately one week to reach levels above MQL (McLagan et al., 2016b). A PAS with yellow

426   Radiello would presumably require deployments twice as long. For either configuration, longer

427   deployments of a month or more are likely to yield greater accuracy. Given the possibility of

428   adjusting the *SR* for the slight effect caused by wind speeds above 1 m s^{-1} and the shorter

429   minimum deployment times, we recommend the PAS configuration with a shielded white

430   Radiello for most outdoor deployments. Nonetheless, there may be long deployments under

431   highly variable winds that warrant the use of the yellow Radiello®. A full long-term calibration

432   study outdoors would be advisable prior to using this configuration.

433   Finally, our results suggest that previously deployed Radiello® are indeed reusable as long as

434   the Radiellos® are cleaned between deployments. Because the different cleaning methods were

435   generally equally effective, we recommend the use of the *soap* method because of its overall

436   ease and health, safety and waste benefits over using acids (Anastas and Warner, 1998).

437   **Data Availability**

438   Data can be found in the paper, the SI, or via communication with the corresponding author.

439   **Competing Interests**

440   The authors declare that they have no conflicts of interest.

Acknowledgements

441

442 We acknowledge funding from Strategic Project Grant #463265-14 by the Natural Sciences and

443 Engineering Research Council of Canada (NSERC) and an NSERC Alexander Graham Bell Canada

444 Graduate Scholarship. We thank S. Steffen of Environment and Climate Change Canada for the

445 loan of the Tekran instrument and B. Branfireun, S. Bartlett, C. Hamilton, and A. Craig from

446 Western University for providing access to the BIOTRON facility.

447 **References**

448 Anastas, P. T., and Warner, J. C.: Green chemistry: Theory and practice, Oxford University Press,

449 New York, USA, 152 pp., 1998.

450 Armitage, J. M., Hayward, S. J., and Wania, F.: Modeling the uptake of neutral organic chemicals

451 on XAD passive air samplers under variable temperatures, external wind speeds and ambient

452 air concentrations (PAS-SIM), Enviro. Sci. Technol., 47, 13546-13554, 2013.

453 Bartkow, M. E., Booij, K., Kennedy, K. E., Müller, J. F., and Hawker, D. W.: Passive air sampling

454 theory for semivolatile organic compounds, Chemosphere, 60, 170-176,

455 http://dx.doi.org/10.1016/j.chemosphere.2004.12.033, 2005.

456 Brown, R. J. C., Kumar, Y., Brown, A. S., and Kim, K.-H.: Memory effects on adsorption tubes for

457 mercury vapor measurement in ambient air: elucidation, quantification, and strategies for

458 mitigation of analytical bias, Environ. Sci. Technol., 45, 7812-7818, 2011.

459 Brown, R. J. C., Burdon, M. K., Brown, A. S., and Kim, K.-H.: Assessment of pumped mercury

460 vapour adsorption tubes as passive samplers using a micro-exposure chamber, J. Environ.

461 Monitor., 14, 2456-2463, 10.1039/C2EM30101F, 2012.

462 Cole, A. S., and Steffen, A.: Trends in long-term gaseous mercury observations in the Arctic and

463 effects of temperature and other atmospheric conditions, Atmos. Chem. Phys., 10, 4661-4672,

464 10.5194/acp-10-4661-2010, 2010.

465 Driscoll, C. T., Mason, R. P., Chan, H. M., Jacob, D. J., and Pirrone, N.: Mercury as a global

466 pollutant: sources, pathways, and effects, Environ. Sci. Technol., 47, 4967–4983, 2013.

467   Guo, H., Lin, H., Zhang, W., Deng, C., Wang, H., Zhang, Q., Shen, Y., and Wang, X.: Influence of

468   meteorological factors on the atmospheric mercury measurement by a novel passive sampler,

469   Atmos. Environ., 97, 310-315, 2014.

470   Gustin, M. S., Lyman, S. N., Kilner, P., and Prestbo, E.: Development of a passive sampler for

471   gaseous mercury, Atmos. Environ., 45, 5805-5812,

472   http://dx.doi.org/10.1016/j.atmosenv.2011.07.014, 2011.

473   Huang, J., Lyman, S. N., Hartman, J. S., and Gustin, M. S.: A review of passive sampling systems

474   for ambient air mercury measurements, Environ. Sci. Process. Impacts, 16, 374-392, 2014.

475   Lozano, A., Usero, J., Vanderlinden, E., Raez, J., Contreras, J., and Navarrete, B.: Air quality

476   monitoring network design to control nitrogen dioxide and ozone, applied in Malaga, Spain,

477   Microchem. J., 93, 164-172, http://dx.doi.org/10.1016/j.microc.2009.06.005, 2009.

478   McLagan, D. S., Mazur, M. E. E., Mitchell, C. P. J., and Wania, F.: Passive air sampling of gaseous

479   elemental mercury: a critical review, Atmos. Chem. Phys., 16, 3061-3076, 10.5194/acp-16-3061-

480   2016, 2016a.

481   McLagan, D. S., Mitchell, C. P. J., Huang, H., Lei, Y. D., Cole, A. S., Steffen, A., Hung, H., and

482   Wania, F.: A High-Precision Passive Air Sampler for Gaseous Mercury, Environ. Sci. Technol.

483   Lett., 3, 24-29, 10.1021/acs.estlett.5b00319, 2016b.

484   McLagan, D. S., Huang, H., Lei, Y. D., Wania, F., and Mitchell, C. P. J.: Prevention of catalyst

485   poisoning in automated atomic absorption spectroscopy instruments for analysis of total

486   mercury samples with high sulphur content, Submitted to: Spectrochim Acta B, 2017.

487   Moeckel, C., Harner, T., Nizzetto, L., Strandberg, B., Lindroth, A., and Jones, K. C.: Use of

488   depuration compounds in passive air samplers: Results from active sampling-supported field

489   deployment, potential uses, and recommendations, Environ. Sci. Technol., 43, 3227-3232, 2009.

490   New, M., Lister, D., Hulme, M., and Makin, I.: A high-resolution data set of surface climate over

491   global land areas, Climate research, 21, 1-25. URL of data:

492   https://crudata.uea.ac.uk/cru/data/hrg/tmc/, 2002.

493   Pennequin-Cardinal, A., Plaisance, H., Locoge, N., Ramalho, O., Kirchner, S., and Galloo, J.-C.:

494   Performances of the Radiello® diffusive sampler for BTEX measurements: Influence of

495   environmental conditions and determination of modelled sampling rates, Atmos. Environ., 39,

496   2535-2544, http://dx.doi.org/10.1016/j.atmosenv.2004.12.035, 2005.

497   Peterson, C., Gustin, M., and Lyman, S.: Atmospheric mercury concentrations and speciation

498   measured from 2004 to 2007 in Reno, Nevada, USA, Atmos. Environ., 43, 4646-4654,

499   http://dx.doi.org/10.1016/j.atmosenv.2009.04.053, 2009.

500   Pirrone, N., Cinnirella, S., Feng, X., Finkelman, R., Friedli, H., Leaner, J., Mason, R., Mukherjee,

501   A., Stracher, G., and Streets, D.: Global mercury emissions to the atmosphere from

502   anthropogenic and natural sources, Atmos. Chem. Phys., 10, 5951-5964, 2010.

503   Plaisance, H., Sagnier, I., Saison, J., Galloo, J., and Guillermo, R.: Performances and application

504   of a passive sampling method for the simultaneous determination of nitrogen dioxide and

505   sulfur dioxide in ambient air, Environ. Monitor. Assess., 79, 301-315, 2002.

506   Plaisance, H., Piechocki-Minguy, A., Garcia-Fouque, S., and Galloo, J. C.: Influence of

507   meteorological factors on the NO2 measurements by passive diffusion tube, Atmos. Environ.,

508   38, 573-580, http://dx.doi.org/10.1016/j.atmosenv.2003.09.073, 2004.

509   Plaisance, H.: The effect of the wind velocity on the uptake rates of various diffusive samplers,

510   International Journal of Environmental Analytical Chemistry, 91, 1341-1352,

511   10.1080/03067311003782625, 2011.

512   Restrepo, A. R., Hayward, S. J., Armitage, J. M., and Wania, F.: Evaluating the PAS-SIM model

513   using a passive air sampler calibration study for pesticides, Environ. Sci. Process. Impacts, 17,

514   1228-1237, 2015.

515   Rutter, A. P., Snyder, D. C., Stone, E. A., Schauer, J. J., Gonzalez-Abraham, R., Molina, L. T.,

516   Márquez, C., Cárdenas, B., and de Foy, B.: In situ measurements of speciated atmospheric

517   mercury and the identification of source regions in the Mexico City Metropolitan Area, Atmos.

518   Chem. Phys., 9, 207-220, 10.5194/acp-9-207-2009, 2009.

519   Selin, N. E.: Global biogeochemical cycling of mercury: a review, Annu. Rev. Env. Resour., 34, 43-

520   63, doi:10.1146/annurev.environ.051308.084314, 2009.

521   Shoeib, M., and Harner, T.: Characterization and comparison of three passive air samplers for

522   persistent organic pollutants, Environ. Sci. Technol., 36, 4142-4151, 2002.

523   Skov, H., Sørensen, B. T., Landis, M. S., Johnson, M. S., Sacco, P., Goodsite, M. E., Lohse, C., and

524   Christiansen, K. S.: Performance of a new diffusive sampler for Hg0 determination in the

525   troposphere, Environ. Chem., 4, 75-80, http://dx.doi.org/10.1071/EN06082, 2007.

526   Steffen, A., Douglas, T., Amyot, M., Ariya, P., Aspmo, K., Berg, T., Bottenheim, J., Brooks, S.,

527   Cobbett, F., Dastoor, A., Dommergue, A., Ebinghaus, R., Ferrari, C., Gardfeldt, K., Goodsite, M.

528   E., Lean, D., Poulain, A. J., Scherz, C., Skov, H., Sommar, J., and Temme, C.: A synthesis of

529   atmospheric mercury depletion event chemistry in the atmosphere and snow, Atmos. Chem.

530   Phys., 8, 1445-1482, 10.5194/acp-8-1445-2008, 2008.

531   Steffen, A., Scherz, T., Olson, M., Gay, D., and Blanchard, P.: A comparison of data quality

532   control protocols for atmospheric mercury speciation measurements, J. Environ. Monitor., 14,

533   752-765, 2012.

534   UNEP: Minamata Convention on Mercury: Text and Annexes, United Nations Environmental

535   Programme, Geneva, Switzerland, 67, 2013.

536   USEPA: Method 7473: Mercury in solids and solutions by thermal decomposition,

537   amalgamation, and atomic absorption spectrophotometry, United States Environmental

538   Protection Agency, Washington, 17, 2007.

539   Zhang, W., Tong, Y., Hu, D., Ou, L., and Wang, X.: Characterization of atmospheric mercury

540   concentrations along an urban–rural gradient using a newly developed passive sampler, Atmos.

541   Environ., 47, 26-32, http://dx.doi.org/10.1016/j.atmosenv.2011.11.046, 2012.

542   Zhang, X., Brown, T. N., Ansari, A., Yeun, B., Kitaoka, K., Kondo, A., Lei, Y. D., and Wania, F.:

543   Effect of wind on the chemical uptake kinetics of a passive air sampler, Environ. Sci. Technol.,

544   47, 7868-7875, 2013.